Modal sequencing and dynamic emission properties of an 8-h Giant Metrewave Radio Telescope observation of pulsar B1822−09

Crystal Latham,[1][⋆] Dipanjan Mitra[2][⋆] and Joanna Rankin[1,3][⋆]

[1]*Physics Department, University of Vermont, Burlington, VT 05405, USA*
[2]*National Centre for Radio Astrophysics, Ganeshkhind, Pune 411 007, India*
[3]*Sterrenkundig Instituut 'Anton Pannekoek', University of Amsterdam, NL-1090 GE Amsterdam, the Netherlands*

ABSTRACT

The research presented here examines an 8-h observation of pulsar B1822−09, taken by the Giant Metrewave Radio Telescope. B1822−09 has been known to exhibit two stable emission modes, the B-mode, where the precursor (PC) 'turns-on', and the Q-mode, which is defined by interpulse (IP) emission. The results of our analysis, of this extremely long observation, have shown that B1822−09 exhibits at least three other emission behaviours that have not been seen before in other similar pulsars or in other observations of B1822−09. These three behaviours can be described as Q-mode emission with PC emission, B-mode emission with IP emission and instances where both the PC and IP are 'on' when transitioning from one mode to the other. The pulse structure has been found to be more complex than previously thought. The main pulse (MP) has an inner cone/core triple (T) configuration together with a central sightline traverse. The IP is a $15°$-wide region that along with the MP originate from an open dipolar field. The PC emission comes from a still unknown source. We argue that the PC emission arises within the same region as the MP, but likely comes from higher in the magnetosphere. The Q-mode has a very clear fluctuation that occurs in both the MP and IP at 46.6-P_1 which is associated with drifting subpulses. Furthermore, we have found that the B-mode, which has previously never shown any detectable modulations at this radio frequency, has a very weak feature at 70-P_1. Coincidently we find the ratio of the B-mode 'P_3' of 70-P_1 to its Q-mode counterpart of 46.6-P_1 is very nearly 3/2, which seems to imply a carousel of three MP 'sparks' in the Q-mode and two sparks in the B-mode. The circulation times of the two modes have been found to be virtually equal at 140-P_1, which allows for this interpretation of the fluctuation features as 'sparks'. Overall, our analyses strongly suggest that mode changes allow information transfer between the two magnetic polar regions and contribute to global magnetospheric changes.

Key words: pulsars: general – pulsars: individual: B1822−09.

1 INTRODUCTION

Radio pulsar B1822−09's fascinating characteristics have attracted the attention of many investigators who have described aspects of its modal and pulse-sequence (PS) behaviour. In this paper, we present new analyses of B1822−09, based on one of the longest observations ever recorded by the Giant Metrewave Radio Telescope (GMRT). Most existing studies of the pulsar's PSs had relied on observations carried out at frequencies higher than 1 GHz (e.g. Fowler & Wright 1982) – apart, that is, from our recent 325-MHz GMRT

effort reported by Backus, Mitra & Rankin (2010, hereafter Paper I) and a just published, comprehensive low-frequency analysis by Suleymanova, Logvinenko & Smirnova (2012, hereafter SLS12). In this more extensive investigation of B1822−09's emission characteristics, we are able to extend – and in some cases correct – Paper I conclusions.

Pulsar B1822−09 is known to exhibit three interesting phenomena simultaneously: two 'modes' in its average pulse profile, interpulse (IP) emission and periodic subpulse modulation (Fowler, Morris & Wright 1981; Morris et al. 1981; Fowler & Wright 1982). B1822−09 switches between its 'Q'uiescent and its 'B'urst modes (Fowler et al. 1981; Gil et al. 1994). Some studies have reported that mode changes occur approximately every 5 min (e.g. Fowler & Wright 1982); however, our observations show that both modes

can at times persist for much longer intervals. The Q-mode exhibits an IP located about half a rotation period (hereafter P_1) from the main pulse (MP), which shows strong low-frequency modulation at some 43 P_1. The B-mode, by contrast, exhibits a brighter and more complex MP as well as a precursor (PC) component some 15° longitude prior to the MP, but no detectable IP. Indeed, B-mode profiles suggest a connecting 'bridge' between the PC and MP.

The half-period-separated IP of B1822−09 suggests that the pulsar may have an orthogonal geometry, where the MP is radiated above one magnetic pole and the IP above the other (Gil et al. 1994). As discussed in Paper I, earlier investigators had regarded the PC and MP as a pair of features – a conal double structure whose leading portion was present or absent in the two modes and whose centre point trailed the bright IP feature by a little less than half a period. However, some have argued that the PC and IP are emitted by the same emission region, which reverses emission direction in its two modes (Dyks, Zhang & Gil 2005); whereas others have suggested a purely geometrical model for the profile of B1822−09 (Petrova 2008).

In Paper I, we departed from the view that the PC and MP constitute a pair. We found that the MP has three partially merged features, and that these have the expected angular dimensions for an inner-cone/core triple (T) profile, viewed in a nearly orthogonal sightline geometry (see also ET VI; Rankin 1993a,b). Our sensitive observations also showed that the IP has what is probably a conal double (D) structure, rather than the single feature seen previously – and that the midpoints of the IP and MP are separated by almost exactly 180°. In summary, the evidence appears very strong indeed that the IP and MP are emitted above the star's two magnetic poles, though this understanding leaves the PC without any ready interpretation within the core/double-cone model.

Previous studies of B1822−09 give the impression that the two modes each appear roughly half of the time. However, one of the PSs described in Paper I consisted of an unusually long (2106-pulse) Q-mode observation; whereas in the other the longest B-mode interval was only 255 pulses. In this analysis, we have acquired an 8-h, 37 399-pulse GMRT observation of which approximately 10 per cent or 3740 pulses were omitted from analysis owing either to radio frequency interference (RFI) or telescope phasing. Investigation of the remaining 33 000+ pulses have provided a number of new opportunities. Indeed, the observation includes the longest Q-mode PS ever recorded, a total of 7200 pulses as well as a B-mode interval some 1050 pulses in length, four times longer than was available to Paper I.

Our unprecedentedly long metre-wavelength observation provides an opportunity to ask new questions about the character of B1822−09's emission. In terms of sequencing, we find brief instances when the modes appear to be in transition as well as instances where the PC and IP appear simultaneously. We have also found that the PC, IP and MP have multiple features within their profile structure, which can be intercompared and interpreted. On close inspection, the MP intensity varies considerably, and at times almost nulls, such that both the IP and PC are undetectable. The several long unimodal PSs facilitate detailed fluctuation-spectral analyses, and in particular we find a long period Q-mode modulation feature common to both the MP and IP for the first time. Finally, we use the results of the analyses to assess current models pertaining to the emission geometry and characteristics of this pulsar.

In Section 2, we describe the GMRT observation of B1822−09, and in Section 3, we discuss the modal profile characteristics of the pulsar, including its pulse structure, MP emission and the pulse-intensity variations with time. Section 4 addresses the pulsar's moding behaviours; while in Section 5 we present the results of our fluctuation-spectral analyses. In Section 6, we summarize our main findings and their implications, as well as discuss how these results should be interpreted in the context of the various theoretical interpretations of B1822−09's emission properties.

2 OBSERVATION

The 8-h, 325-MHz observation of B1822−09 provides the basis for our analyses in this paper. The observations were carried out at the GMRT near Pune, India. The GMRT is a multi-element aperture-synthesis telescope (Swarup et al. 1991) consisting of 30 antennas distributed over a 25-km-diameter area which can be configured as a single dish both in coherent and incoherent array modes of operation. For these observations we used the coherent (or more commonly known as phased-array) mode of the GMRT. A bandwidth of 16 MHz was used (whole band running from 325 to 341 MHz) and the data were recorded using the GMRT pulsar machine at a time resolution of 0.512 ms. The observations used 20 GMRT antennas (14 central square and two each in the east–west and south arms) for phasing. Usually the calibrator source used for phasing lies several degrees away from the pulsar and one needs to rephase the array every 1.5 h which causes missing pulsar-less time sections in the data. However, for this observation the phase calibrator used was 1822−096 lying in the same primary beam of the telescope, and hence phasing could be done while the pulsar was always on the beam. This way we were able to record 37 399 continuous pulses almost without breaking the pulsar data stream. Only between pulse number 14 016 to 14 910 due to interference the telescope was slewed to a nearby calibrator source for checking the phasing.

After dedispersion most of the data were of good quality. However, in sections there were large baseline variations due to broadband interference. This was mostly mitigated by running mean subtraction of the baselines as well as flattening of the baseline for every single pulse. No significant power line RFI was present in the dedispersed data stream.

3 MODAL BEHAVIOUR

Pulsar B1822−09's modal effects are among of its most fascinating and important behaviours. Following the convention of earlier investigators, we discuss its modes in terms of its 'quiescent' Q- and 'bright' B-modes. The Q-mode is by far the most usual mode; it persists through 60 per cent of our observation. The longest (very nearly) continuous Q-mode apparition is 7201 pulses long, which is shown in the upper portion of Fig. 1. By contrast, the B-mode persists for only 30 per cent of the observation, and its longest continuous apparition is 1151 pulses in length, shown in the lower portion of Fig. 1. These two modes define the emission from B1822−09, and in our observation we have discovered that these two modes occur in parallel to create three other behaviours: Q-mode with PC activity (Qw/PC), B-mode with IP activity (Bw/IP) and both together at modal transitions.

3.1 Parallel moding

Looking closely at the bottom B-mode display of Fig. 1, an obvious low level of IP emission can be discerned at the beginning of this long sequence. Nearly all intervals of consistent B-mode emission, some 93 per cent, also contain instances of IP emission. Similarly, in the upper Q-mode display, an interval can be seen around pulse
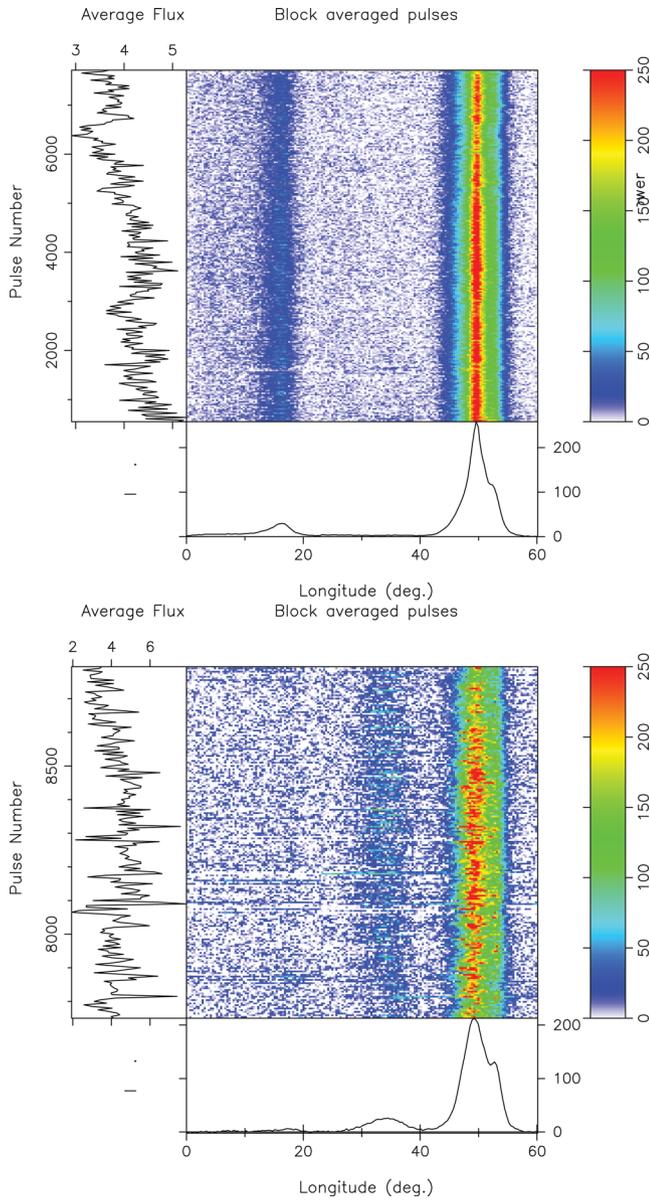
Figure 1. Top: display of the longest, 7200-pulse Q-mode interval (pulses 20 550–27 750) in 29-pulse subaverages (main panel); aggregate intensity (left-hand panel) and total average profile (bottom panel). The first 10° of longitude have been removed, and a further 140° have been removed at +23° (as in Paper I), so that all three regions of the profile can be seen at once. Note the IP, relatively narrow MP and the lack of the PC. Bottom: display of the longest, 1050-pulse B-mode interval (pulses 27 750–28 800) in five period averages as above. Note the broader, more complex MP, the PC and weak IP. Here, the pulses number from 20 000.

21 620 where the B-mode appears to flicker 'on' for a few pulses. The former is just one clear instance wherein the usually mutually exclusive PC and IP are found to occur simultaneously. At other times both the IP and PC seem to be 'off' briefly – but this might be expected because in the Q-mode the IP is cyclical. Overall, we have found it challenging to fully characterize as long an observation as the present one at the single-pulse level; however, it is very clear that the two modes are not as 'pure' as previously thought. Such instances tend to occur during transitions between the modes (see e.g. Fig. 2), though the above examples occur well into long modal intervals.
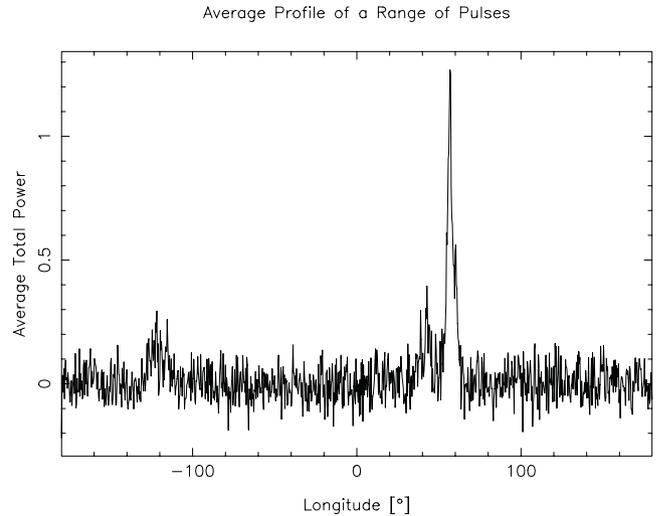

Figure 2. Four-pulse average profile (20 548–20 551) showing the transition region to the long Q-mode apparition in Fig. 1 (upper). Here we see a good example of simultaneous IP and PC illumination.

Moding 'in parallel' – that is, simultaneous IP and PC activity – is a phenomenon that had not previously been identified in pulsar B1822−09. In the foregoing example, IP emission occurred within an otherwise ordinary B-mode interval, so one might dub the effect B-mode with IP (or Bw/IP), and indeed this the most common form of parallel moding. About 29 per cent of the pulses in our observation have been classified as the Bw/IP mode. Though not nearly as common, the Q-mode with PC (Qw/PC) also occurs throughout our observation in about 11 per cent of the pulses. The Qw/PC intervals are identified by PC emission within an otherwise normal Q-mode PS. Finally, a third type of parallel moding sometimes occurs when B1822−09 transitions from B to Q or vice versa.

3.2 Modal sequencing

B1822−09 is known for its unique modal sequencing, and with our extremely long observation we were able to see changes and patterns of moding throughout. Fig. 3 gives a diagram summarizing the modal configuration over the entire observation. Noisy areas of the observation have been integrated into the respective modal sequence in which it occurs to simplify the presentation. The most common pattern is for the modes to alternate from Q to Bw/IP and
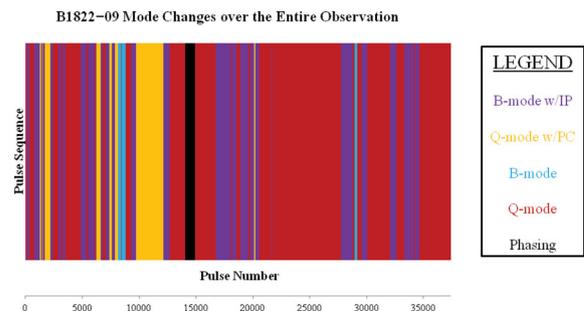

Figure 3. Modal sequencing in the 8-h (37 399 pulse) GMRT observation. The Q-mode occurs more often and in longer intervals than the B-mode. Also, the IP 'sputters on' in B-mode intervals (Bw/IP) and the PC in Q-mode sections (Qw/PC). Alternating intervals of Q and Bw/IP are also noticeable (seen as red and purple patterns). The black region corresponds to the time section used for phasing the antenna.

back to Q. In this specific pattern, the transition typically has a duration of a few pulses. A few instances of Bw/IP to Qw/PC and back to Bw/IP were also identified. Interestingly, the two longest intervals of relatively pure Q- and B-mode occur together, right after one another. Previous studies had found that mode switching occurs approximately every 5 min (e.g. Fowler & Wright 1982); however, here we have found that the average time between mode changes is about 7.6 min, or a pulse length of 593 pulses.

4 AVERAGE PROFILE STRUCTURE

Pulsar B1822−09's MP, PC and IP have long been studied, but only recently has a full and consistent picture of these structures emerged. Here, we have the benefit of long continuous B- and Q-mode intervals, which we find confirm and extend the viewpoints developed in Paper I. Fig. 1 (upper display) shows the longest Q-mode interval, 7201 pulses, in 29 period averages, spanning pulses 20 550–27 750; whereas, Fig. 1 (lower) shows the longest B-mode sequence, from pulse 27 750 to 28 800, in five period averages. We can see clearly again here that the MP amplitude is similar in the two modes, so that the B-mode is largely brighter due to its increased width.

4.1 Modal profile structure

Paper I argued that the MP was composed of three poorly resolved features, and that it reflected a nearly orthogonal (magnetic latitude α about 90°) inner cone/core triple (T) configuration together with a central sightline traverse (impact angle β near 0°). Using the long B- and Q-mode intervals in this observation, we have computed peak-occurrence histograms (not shown) for the MP in both modes. Unsurprisingly, these show sharp peaks at sample 674 (of 1024), but also the broad leading and trailing pedestals indicative of a triple structure. The mixed-mode structure of the MP is remarkably similar within the two octaves below 1.6 GHz (e.g. Gould & Lyne 1998), and SLS12 show that this basic structure persists with some broadening down to 62 MHz.

Fig. 4 (upper) exhibits the pulsar's Q-mode profile structure using correlation maps: leading and trailing regions of the MP correlate both with each other and the IP; whereas, the central region of the MP shows correlation only with itself. The corresponding B-mode correlations are then shown in Fig. 4 (lower), and the difference could not be more marked. Here we see negligible correlation both between the MP regions as well as with the PC.

Further, Paper I showed that the IP extended 10° or so earlier than the single trailing peak seen at higher frequencies. In our observation that peak occurs at sample 179, so that the interval between the MP and IP peaks is indeed the often quoted 186°. However, the IP midpoint lies 6°–7° earlier, so that the MP and IP profile centres are almost exactly half a period apart. Had there been any lingering doubt about this interpretation, SLS12's remarkable 62-MHz IP detection – showing a symmetrical dual-lobed IP (their fig. 6) – resolves it. They also show that its 62-MHz midpoint follows the MP peak by almost exactly 180°, which together with (corrected) high frequency measurements (Hankins & Fowler 1986) show that the MP–IP separation is constant within small uncertainties over the entire range of available observations. Finally, SLS12's fig. 7 shows that the MP and IP profile widths are comparable and escalate comparably in a conal fashion.

Longitude–longitude correlation plots confined to the IP (not shown) further elucidate its structure. Only the region around the peak is correlated with itself at either 0- or 1-pulse delay. Similar
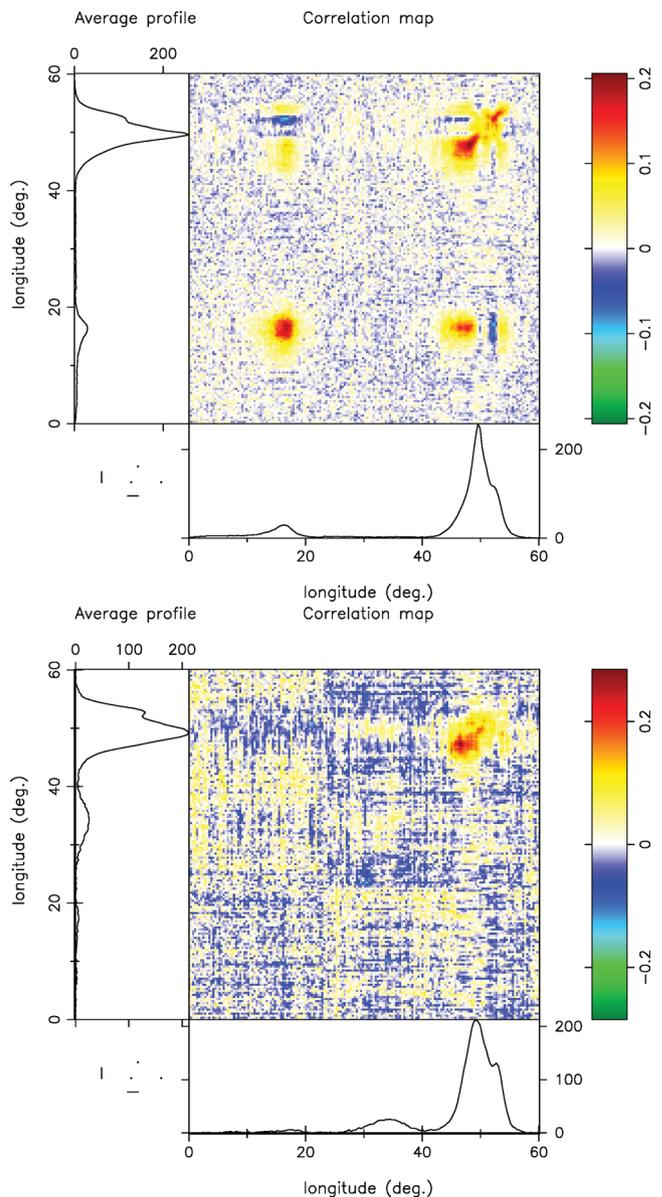

Figure 4. Longitude–longitude correlation displays at one-pulse lag corresponding to the long Q- (upper) and B-mode (lower) intervals in Fig. 1. In the Q-mode, the MP correlates substantially both with itself and the IP. Indeed, the leading, centre and trailing parts of the MP exhibit different amounts and types of correlation, demonstrating its triple character. Only the IP peak correlates, but the remainder is probably too weak for this analysis. However, the B-mode self-correlation in the MP, its cross-correlation with the PC and the PC's self-correlation are weak to negligible. The contrast with the Q-mode could not be more marked. The 3σ errors on the correlations here are 0.035 and 0.093, respectively.

displays computed for lags of 23- and 46/47-P_1 show comparable levels of negative and positive correlation, respectively – and again no perceptible correlation with the early part of the IP.

The foregoing understanding of the MP and IP then leaves the PC without any plausible interpretation within the double-cone/core model. As emphasized in Paper I, its large fractional polarization and shallow polarization position angle (PPA) traverse contrast sharply with the MP and IP. Its Gaussian-shaped, single form peaks in our observation at sample 631 with a half-power width of 7°.0, thus leading the MP peak by 15°.1 – and reference to high-frequency
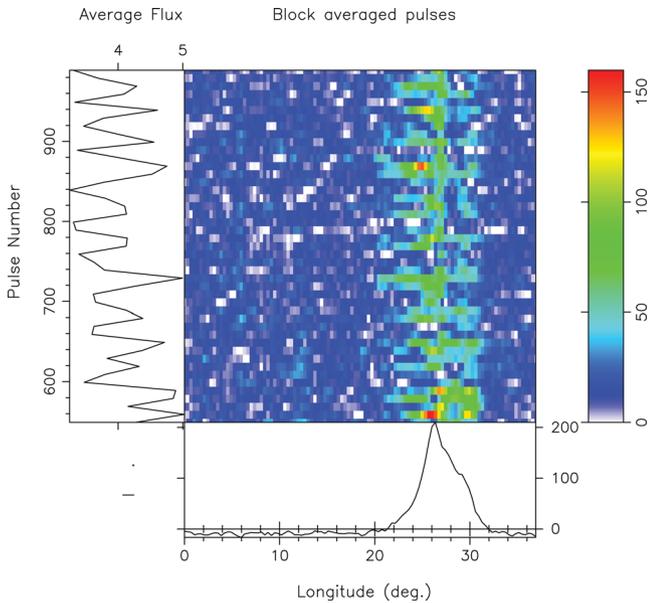
Figure 5. Beginning of the long Q-mode PS in Fig. 1 in 10-pulse averages. Here we see clearly that emission associated with the trailing part of the profile decreases.

profiles (e.g. Gould & Lyne's 1998 at 1.6 GHz) shows a virtually identical form and spacing. The PC's radio frequency (RF) spectrum is substantially flatter than that of the other components as can be seen in Gould & Lyne's (1998) profiles, and this trend continues at low frequencies where only hints of the PC are seen in SLS12's decimetre profiles. We also attempted to explore the PC's structure using correlation analyses (e.g. Fig. 4, lower), but the feature self-correlates only narrowly and shows negligible pulse-to-pulse correlation.

4.2 Secular changes in pulse intensity

Paper I noted a secular decrease in the amplitude of the two main component peaks during the early part of a Q-mode sequence (their fig. 14), and this effect was interesting because it seemed to mirror what had been seen earlier in pulsar B0943+10 following its B-mode onset. Here, we have more opportunities to examine the intensity behaviour during both modal episodes of the profile. Fig. 5 shows the beginning of the long Q-mode sequence of Fig. 1 (upper) in 10-pulse averages, and we see clearly that the intensity of the trailing component diminishes over the first 100 or so pulses. Indeed, given that in general the B-mode PSs are more intense that those of the Q-mode – and that such intensity changes occur at the modal transition – we might regard this excess power in the trailing component as 'left over' from the preceding B-mode. Systematic intensity changes are also seen in the B-mode sequences. Fig. 6 shows a series of short B-mode episodes between pulses 4501 and 10 000. First, a dramatic intensity increase in the early part of the MP coincides with the beginning of each B-mode episode, and secondly, the overall intensity (left-hand panel) is seen to fall off during most of the B-mode intervals.

5 FLUCTUATION-SPECTRAL ANALYSES

Pulsar B1822−09's prominent 43-P_1 Q-mode fluctuation feature is well known from earlier studies (e.g. Paper I). It modulates the IP peak as well as both leading and trailing regions of the MP. However, a fluctuation cycle this long is difficult to measure accurately, so
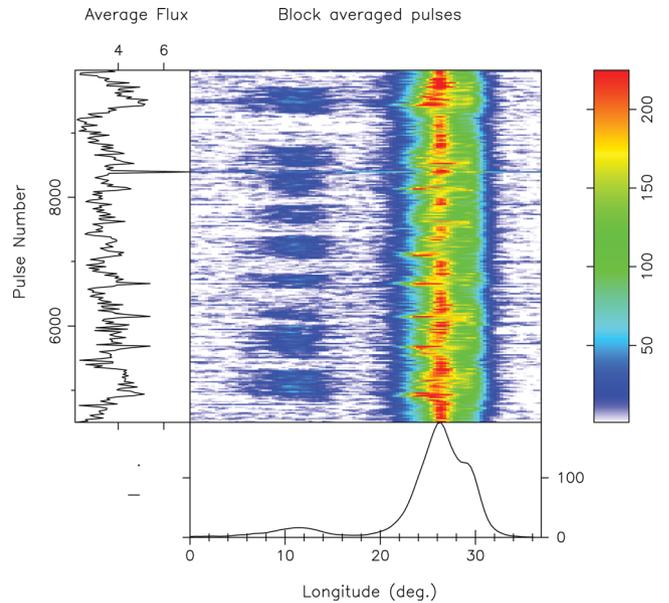

Figure 6. B-mode episodes during pulses 4501–10 000 in 22-pulse averages. Note the strong emission on the leading edge of the MP that coincides with the beginning of each B-mode interval. Also, the average flux (left-hand panel) decreases markedly during each apparition. The strong response near pulse 8400 is RFI.

little is known about its precise frequency, possible variations or behaviour near modal transitions. Earlier studies using 256-length fast Fourier transforms (FFTs) entail a half-bin error or $\pm 3.5\,P_1$, so the 43-P_1 value must be considered a nominal one.

5.1 Q-mode modulation frequency

Here, the very long observation and unprecedentedly long Q-mode intervals provide a possibility of improved precision and better answers to the above question. In particular, Fig. 7 shows longitude-resolved fluctuation (LRF) spectra for the longest Q-mode apparition in Fig. 1 (upper). Using a 1024-length FFT, all the fluctuation power falls in a single bin; whereas, in an FFT of twice this length the power is divided about equally between two bins. Thus the modulation period and uncertainty can be given as $46.55 \pm 0.88\,P_1$.

Over the duration of the longest Q-mode interval, we found that the strength of the modulation varied greatly, but no deviation from this period could be discerned. For instance, Fig. 8 gives LRF spectra for the most highly modulated region near the centre of the Q-mode apparition (pulses 23 622–24 645). Here again, all the modulation power is in one bin, so its period and error is as above. Overall, the strength of this modulation seemed to grow stronger during the first half of the apparition and diminish in the latter half. Near the end, just before the B-mode onset (e.g. pulses 26 727–27 750), the feature was very weak and the fluctuation power divided between the two adjacent bins in a 1024-length FFT, but the feature period was indistinguishable from the above, within its larger error.

Our 8-h observation provided a number of other opportunities to measure the Q-mode modulation frequency, but not for as long a continuous sequence as the one above. Other extended such intervals were found roughly between pulses 3500 and 4800, 10 300 and 12 100, 12 700 and 14 000, 14 900 and 16 700, 30 050 and 31 250 and after 34 500. In each of these, the modulation feature was easily seen in both the IP and MP, but was less coherent than in the most stable intervals above. Usually the fluctuation power was divided
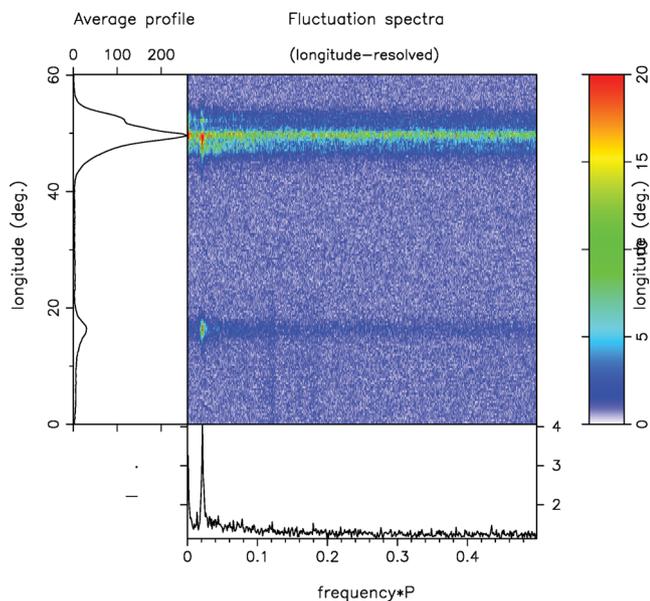
Figure 7. LRF spectra for the longest Q-mode interval in Fig. 1 (upper; pulses 20 550–27 750), using a 1024-point FFT. The MP is at the top and the IP at the bottom of the left-hand panel. The strong feature at about 0.021 cycles period^{-1} (hereafter c/P_1) modulates both the MP and the IP and is coherent here but not using a 2048-length FFT; thus, it corresponds to a P_3 of 46.6 P_1 with an uncertainty of about ± 0.9 P_1. The nature of P_3 will be discussed and interpreted in Section 5.5.
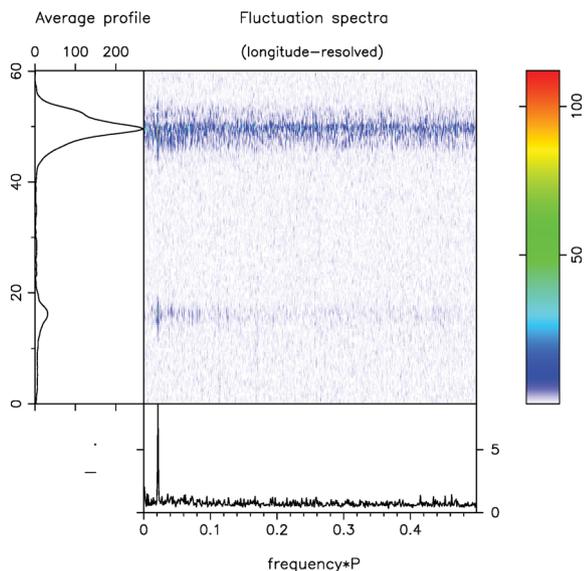

Figure 8. LRF spectra as in Fig. 7 for a highly modulated region near the centre of the long Q-mode apparition (pulses 23 622–24 645) using a 1024-length FFT.

between two bins in a 512-length FFT; however, its period was always comparable to the value above and within its error.

5.2 Character of the Q-mode modulation

We have seen above that both the IP and MP are modulated at the same period and that their fluctuations are highly correlated (e.g. Fig. 4). However, it is important to know in detail just where and how the intensities vary. The display of Fig. 9 then shows a modulation-folded PS of the most coherent region of the longest Q-
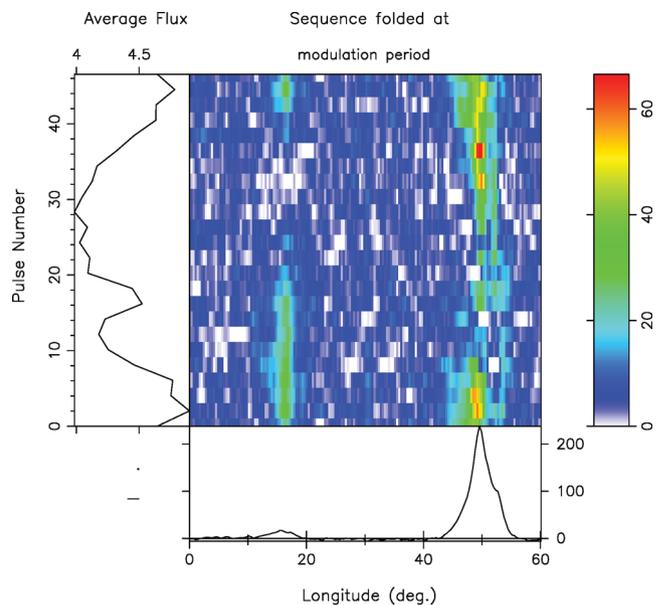

Figure 9. Folded PS of the highly modulated Q-mode region in Fig. 8 with the non-fluctuating 'base' (shown in the bottom panel) removed. We see here that the IP remains stationery in longitude throughout the modulation cycle, whereas the MP fluctuates in a highly ordered and 'drifting' manner.

mode apparition in Fig. 8. Here the non-fluctuating 'base' (bottom panel) has been removed, so only that part of the power that fluctuates is shown. Clearly, the IP fluctuates in a longitude-independent manner; whereas, the MP exhibits a complex behaviour over the course of the modulation cycle.

Taking the IP first for a more detailed analysis, we produced a modfold similar to Fig. 9 restricted to the IP by itself (not shown), and we saw again that the modulation is longitude independent and upwards of 50 per cent modulated (note the range of values in the left-hand panel or compare the 'base' amplitude in the lower panel with that of the colour bar). It will not then be surprising that a harmonic-resolved fluctuation (HRF) spectrum corresponding to the LRF in Fig. 8 (not shown) – restricted to the IP – shows the dual features indicative of amplitude modulation. Or what is the same, a modulation-phase analysis (see Fig. 10) for the same interval shows it constant over the IP 'peak' region (and the fluctuation power in the leading IP region is so small that the phase is meaningless). While these results for the 'coherent' interval of Fig. 8 are especially sensitive, we have applied the same analysis to most other Q-mode regions in the observation with virtually identical results.

Now examining the MP in much the same manner, we computed a modfold similar to Fig. 9 restricted to the MP region by itself (not shown). Here we saw that every part of the MP profile fluctuates in a dynamic and longitude-dependent manner. The central region near the peak fluctuates least and in the most stationary manner, as can be inferred from the aggregate-flux variations in the left-hand panel. Also, power near the trailing edge of the profile seems to participate in the cycle at a fixed longitude. The bulk of the fluctuating power, however, moves through the profile from the trailing to the leading side in a kind of 'drift' over roughly half the cycle. This is clearly seen in an HRF (not shown) similar to the LRF of Fig. 7 – but for the MP region on its own – where the fluctuating MP power is seen to represent an almost pure phase modulation.

Again, these dynamic characteristics of the MP modulation are most clearly seen in the highly 'coherent' region of the longest Q-mode apparition. However, we have carried out similar analyses
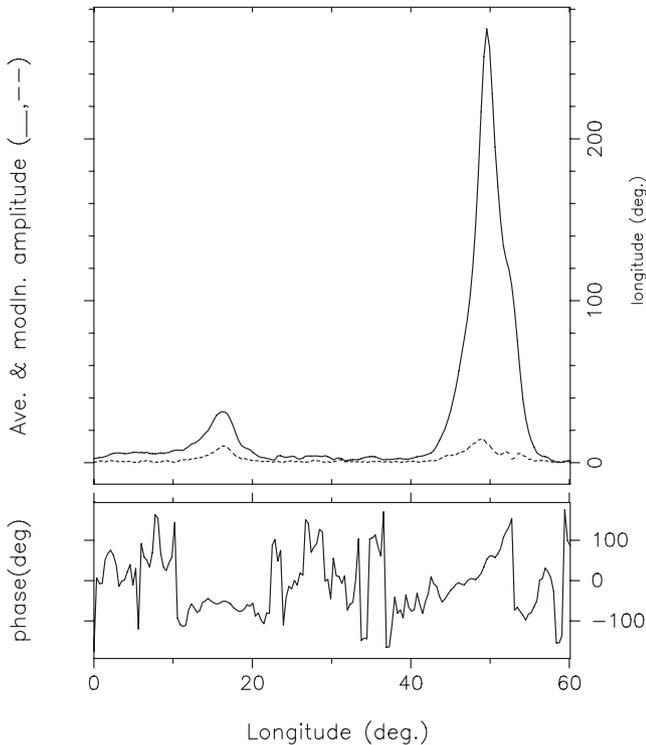
Figure 10. Modulation phase as a function of longitude for the highly modulated Q-mode region in Fig. 8.

Figure 11. The LRF spectra of the longest B-mode sequence, from pulse 27 751–28 800, using a 512 point FFT as in Fig. 7. A strong feature at a period of $70 \pm 3\,P_1$ is evident as well as several more rapid periodicities. The colour-scale is truncated to show the weak features more clearly. During this interval the pulsar flux varies substantially (see Fig. 1), so it was necessary to correct for this possible scintillation.

for each of the shorter Q-mode intervals, and they all seem to behave similarly – that is (a) the peak region exhibits a largely stationary, roughly 10 per cent modulation; (b) a region of stationary fluctuation can be discerned on the trailing edge of the profile just lagging the secondary peak and (c) most of the fluctuation power moves through the profile from the trailing to the leading side during the strong half of the cycle.

Finally, we have seen above that the IP and MP fluctuations are correlated, but it was not fully clear just how. Fig. 10 then gives a partial answer to this question. This modulation-phase diagram includes both the IP and MP, and we see immediately that the IP peak-region phase is stationary whereas the modulation phase under the MP increases with a sharp ramp under most of the profile. Of course, we are dealing here with the phase of a roughly $46\text{-}P_1$ fluctuation, so high temporal precision is impossible. Nonetheless, it is remarkable that the IP is highly correlated (positively) with the leading edge of the MP as well as being both negatively and positively correlated with regions on the MP trailing edge. And this is exactly what appears to be indicated in the 1-period-delay correlation map of Fig. 4.

5.3 B-mode modulation frequency

Fig. 11 gives LRF spectra for the longest B-mode sequence in our observations seen earlier in Fig. 1 (lower). A significant response at a period of about $70 \pm 3\,P_1$ is evident as well as several weaker features. The colour scale was compressed to show the weaker responses more clearly, especially the weak modulation under the PC at about $0.06\,c/P_1$. The $70\text{-}P_1$ feature was not 'coherent' in an FFT of length 1024, but was so using 512; and while strong in the two halves of the PS, it was substantially stronger in the first half. Gil et al. (1994) have reported detecting an $11\text{-}P_1$ feature at higher radio frequencies, but we see no evidence
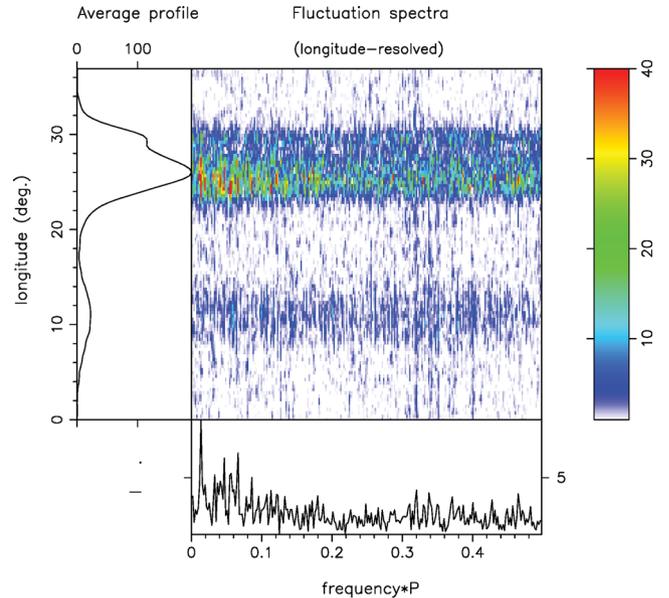
of this in our observation. In only one other section of our observation was another long B-mode apparition available, this in the PS from 16 701 and 17 724; and here no significant periodicity was detected.

5.4 Character of the B-mode modulation

A folded PS of the longest B-mode interval at $70\text{-}P_1$ showed strong corrugation corresponding to an overall modulation depth of about 20 per cent. All parts of the MP were seen to fluctuate as well as a hint that the PC also participated to some degree. Interestingly, a folded PS at twice this period, shown in Fig. 12, exhibited a somewhat larger depth and a suggestion that the PC fluctuations are stronger on alternate cycles. Clearly, we have no other comparable B-mode interval to compare, and the less stable modulation feature in the B-mode prevented our pursuing the analysis further.

5.5 Evidence of carousel circulation

Interestingly, the corrugation in the Q-mode MP folded PS increases significantly at three times the $46.6\text{-}P_1$ feature period. Fig. 13 shows the result, and no other small multiplier of the feature period increased the corrugation noticeably. This suggests that the $46.6\text{-}P_1$ feature should be interpreted as a P_3, not a circulation time (CT).

In fact, where B1822−09's CT found to be as short as $46\text{-}P_1$, interpretation would be awkward, because the pulsar's expected CT, according to Ruderman & Sutherland's (1975, hereafter RS) relation is at least $43\text{-}P_1$, where it as slow in relation to this prediction as most other pulsars with known CTs, it could easily be as long as $250\text{-}P_1$. This is because the pulsar's magnetic field is larger and the period shorter than, for instance, B0943+10.

Therefore, it is interesting to explore whether $3 \times 46.6\text{-}P_1$ or $140\text{-}P_1$ might represent the star's Q-mode CT. By way of exploration we computed a polar map using this putative CT for the
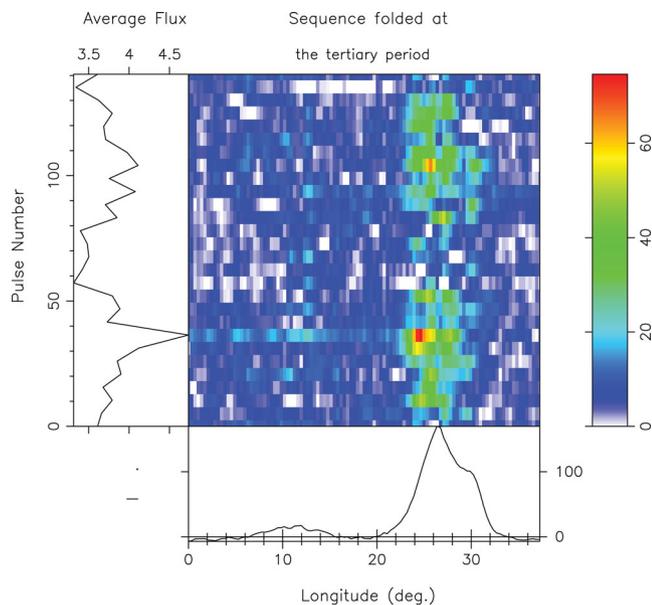
Figure 12. Folded PS of the longest B-mode episode, from pulse 27 751–28 800 as in Fig. 11. A folding period of twice the exact 70-P_1 response was used. All parts of the MP exhibit the 70-P_1 fluctuation, and there is a suggestion that it involves the PC as well. In fact, this modfold suggests that the PC fluctuations are stronger every other 70-P_1 cycle.

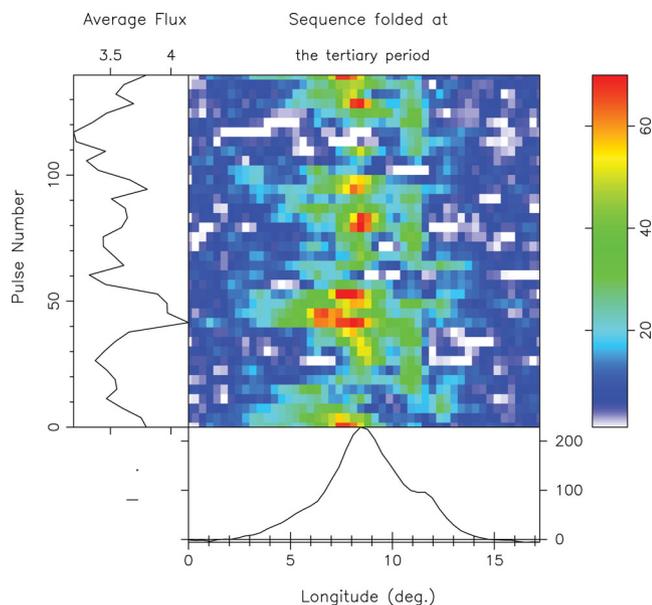**Figure 13.** Folded PS of the Q-mode MP alone as in Fig. 9, but here at three times the 46.6-P_1 cycle. The corrugation is substantially larger, suggesting that this longer cycle is more fundamental.

highly modulated sub-PS of Fig. 8 and the result is shown in Fig. 14. As expected, three broad subbeams can be seen with one somewhat brighter than the others. Given, however, that this map simply reflects the modfold of Fig. 13, it proves nothing by itself. Rather, it provides a means of visualizing how the various correlations computed earlier might be interpreted. Fig. 10 shows that one of the beams, the one on the MP leading edge – correlates in phase with the IP; however, it also indicates that there will be two trailing regions, an inside one that will not correlate in phase and a later one that will. Is this not exactly what we see in the delay-1 correlation map
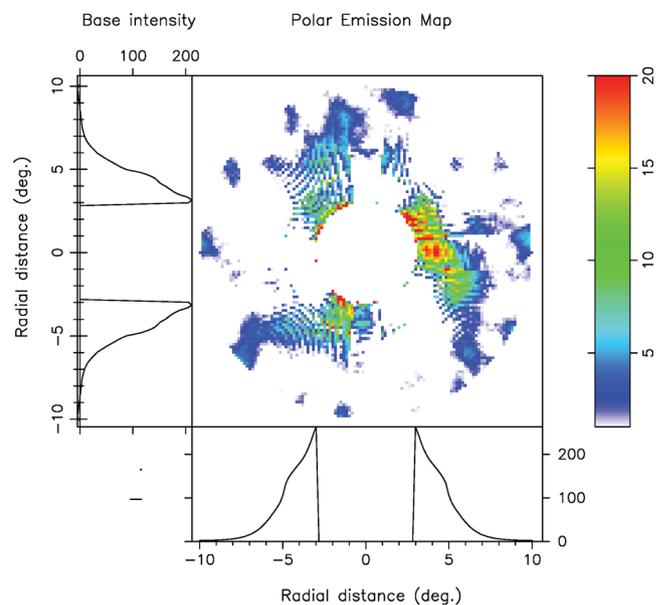

Figure 14. Polar map of the MP subbeam structure in the PS of Figs 9 and 13. A nearly orthogonal geometry where an α and β of 85° and 4°, respectively, was used. It is important to note that the display is not sensitive to the precise values as long as β remains less than about 5°.

of Fig. 4 (upper). Moreover, while the quality of the corresponding B-mode map (lower) is poor, there is no region of negative correlation – as would be expected if there are two rather than three 'beamlets'.

Finally, we note that the periodicities identified in the respective Q- and B-modes appear to be commensurate. The ratio of the B-mode 'P_3' of 70-P_1 to its Q-mode counterpart of 46.6-P_1 is very nearly 3/2. But even more interesting is the appearance that the CTs of the two modes are virtually equal at 140-P_1. If this interpretation is correct, it is the longest (~107.6 s) CT yet identified in any pulsar.

6 SUMMARY AND CONCLUSIONS

Pulsar B1822−09 belongs to a small group of pulsars that have IP emission and is unique in that it also exhibits prominent changes of mode. Moreover, its strongly anticorrelated IP and PC emission have fascinated pulsar investigators and inspired a rich literature. Key, then, to every question is the sources – that is, the magnetospheric geometry of the three corresponding regions of emission.

The recent sensitive, P-band PS observations, however, both above and in Paper I, as well as the 62- and 112-MHz observations by SLS12, clearly demonstrate that the MP is a profile in its own right. Earlier we argued that the MP half-power width of 9°5–10° in both the Q- and B-mode (at around 1 GHz) was consistent with B1822−09 having an inner-cone/core triple (T) profile, and its evolution at low frequency (see SLS12) is compatible with this expectation.

Furthermore, we now find that the IP at metre wavelengths is a roughly 15°-wide region rather than a single feature, with the peak trailing (probably a 'partial cone' as in Mitra & Rankin (2011), hereafter ET IX, terms). The IP's double structure is clearly confirmed in SLS12's 62-MHz profile (their fig. 7), and the overall structure is compatible with an outer conal-double profile, both in its 1-GHz dimension of about 13° ($5°75 \, P_1^{-1/2}$), but also in the manner of its frequency evolution.

Overall, then, we have every indication – on the basis of dimensions, evolution and polarization – that both the MP and IP emission originates from the open dipolar field-line regions, which is true for most other radio pulsars.

The origin of B1822−09's IP emission has long been debated. Early workers had interpreted its 'MP' as being composed of the PC and MP together in the manner of a conal-double profile (notwithstanding the peculiar behaviour of its PC vis-a-vis IP and a raft of other problems with this interpretation). In these terms, the PC–MP centre precedes the IP peak by roughly 186°.

Using, however, the fuller understanding summarized above, the MP centre to IP centre separation is 180° with an error of about ±1° – and apparently invariant over the entire range of available observations. This is just the geometry for which IP emission from the second pole is expected, and indeed this 'orthogonal rotator' two-pole configuration seems to provide the best explanation for the IP emission.

The properties of the PC then contrast strongly with those of the MP and IP as we have seen above, in RF spectrum, polarization, profile evolution and single-pulse properties (e.g. Gil et al. 1994, fig. 6). The location of its region of emission is currently unknown; however, the B1822−09 PC resembles the similar feature in B0943+10 very closely.

In an effort to explain the remarkable anticorrelation between the star's IP and PC emission, Dyks et al. (2005) suggested that the IP and PC emission in fact originate from the same polar region as the MP, but for some reason the IP and PC emission reverse direction during a mode, one emitting in an outward and other in an inward direction. They suggest two kinds of arrangement for this situation. In the first case the IP–PC–MP radiation all comes from the same pole, the PC and MP outwardly and the IP representing the inward emission of the PC. The other configuration has the IP and PC arising from the second pole, where the IP represents outward, and PC inward, emission. Unfortunately, we doubt that this 'downward emission' model is compatible with observations. First, the IP and MP are separated by almost exactly 180°, so a very special design is needed to oppose the IP and PC. Secondly, the PPA traverses below the IP and PC emission are very different (see ET IX); whereas, if they arise from the same diverging field-lines they should be similar. In any case, the displacement due to aberration/retardation (A/R) of twice 300 km or so is only about 1°, so the spacing cannot decide or rule out this conjecture. Thus we believe that the IP and MP emission originate from two magnetic poles and the PC emission is on the MP emission side.

The origin of the PC emission is currently unknown. Given its proximity to the MP, it likely originates above the same pole as the MP and, if associated with the open field of the polar flux tube, then it must be emitted higher in the magnetosphere than the MP. If, for instance, it originates close to the magnetic axis, then an aberration/retardation effect of some 15° corresponds to an emission height of around 5000 km. The properties of the PC emission are very different from those of the MP or IP emission: both the 50 per cent width of the PC feature and its separation from the MP are practically constant over a wide frequency range from 0.3 MHz to 11 GHz (see Gil et al. 1994, fig. 6), whereas the IP and MP emission widths decrease by a factor of 2–2.5 over this band. The PC emission is also highly linearly polarized (Johnston et al. 2008) with a flat PA traverse (e.g. Paper I), suggesting that it may be emitted above the polarization-limiting region (Johnston & Weisberg 2006). Our analysis shows a weak fluctuation spectral feature at $0.06\,c/P_1$ for the PC and also 'spiky' microstructure-like emission with time-scales of about 150 µs as first observed by

Gil et al. (1994). Pre-/post-cursor emission is only seen in a small group of slower pulsars (see ET IX), and does not seem to depend on the pulsar geometry.

B1822−09 is the only interpulsar known to exhibit profile mode changes, and the near anticorrelation of its IP and PC have fascinated pulsarists. During the pulsar's Q-mode, strong, correlated roughly $46\text{-}P_1$ modulation is seen in its IP and MP and the PC is nearly silent; whereas, in the B-mode the IP disappears and PC emission precedes the MP by some 15°, connecting by a low level bridge of emission to the MP. Our study above shows this phenomenon in unprecedented detail. The overall modal sequencing is shown in Fig. 3; whereas, the longest respective Q- (7201 pulses) and B-mode (1026 pulses) subsequences are depicted in the top and bottom displays of Fig. 1, the first showing the IP and MP and the latter the PC and MP.

Interestingly, we have found that the two modes are not as completely 'pure' as formerly thought. We noted earlier that even during the longest Q-mode PS, a few pulses with emission at the PC longitude and a weakening IP can be seen. Or, during the longest B-mode PS, one can see IP emission at a very low (1 per cent) level. This 'flickering' between the two modes seems to be a general phenomenon, and we see short intervals throughout the observation where both the IP and PC are 'on'. Our long sensitive observation allows us to more accurately characterize B1822−09's modal phenomenon. IP emission seems to be present during both B- and Q-mode intervals, but is strong and consistent only in the Q-mode when the PC is absent; otherwise the IP is extremely weak during the B-mode when PC reappears. Modal transitions seem to require a few pulse periods (i.e. a few seconds), and we find many instances where all the three emission features are simultaneously present for short intervals (e.g. see Fig. 2). All this indicates that the mode changes entail changes at both the magnetic poles.

In B1822−09, the strong stable modulation, affecting both the MP and IP, occurs during the Q-mode; here the pulsar is somewhat weaker in intensity, but a more 'perfect drifter' (just the opposite as in B0943+10, where the accurate modulation occurs in the B-mode; see e.g. Paper I). In both pulsars, the appearance of the PC seems to disturb the orderly dynamics of the MP; in B0943+10 the highly regular drift becomes chaotic; in B1822−09 the regular modulation in the leading and trailing conal sections of the MP becomes much less pronounced. Interestingly, the geometries of the two stars could not be more different, in that B0943+10 has a nearly aligned magnetic axis.

Turning now to the fluctuation spectral properties of PSR B1822−09, we found above that the long Q-mode observation exhibited a strong modulation with an apparently constant period of $46.55 \pm 0.88\,P_1$. Further, this fluctuation was seen in both the MP and IP. Both the constant phase of the modulation across the IP region and the HRF indicate that this represents an amplitude modulation of the IP. By contrast, the phase under the MP shows a sharp ramp across the pulse, indicating (together with its HRF) that the fluctuations are largely phase modulated. We have also clearly detected a weak $70 \pm 3\,P_1$ modulation in the longest B-mode sequence; however, no such feature was detected in the other shorter B-mode sequences.

The RS model connects the modulation features of 'drifting' subpulses to 'sparks' undergoing $\boldsymbol{E} \times \boldsymbol{B}$ drift while breaking down the inner vacuum gap. The CT predicted by this model is some $43\text{-}P_1$ which, although close to the observed Q-mode periodicity, should be taken as low by a factor as large as 3 or so – because in virtually every instance where a CT has been determined, it is much longer than that estimated by RS (e.g. for B0943+10 the RS-predicted CT is a factor of 3.5 faster than the observed value). Thus, we interpret

this modulation as a P_3 'drift', not the CT. Indeed, in reaction to the slower observed CTs, Gil, Melikidze & Geppert (2003) predicted that the inner vacuum gap was in fact partially screened by ions, decreasing the electric field and slowing the circulation.

In fact, the CT is related to the parameters of the inner vacuum gap as CT $\sim 2a/\eta$, where η is the screening factor and a is the complexity parameter $a = r_p/h$ which is the ratio of the polar cap radius, r_p, and the vacuum gap height, h (see equation 11 of Gil & Sendyk 2000, and equation A1 of Gil et al. 2008). Assuming the screening factor[1] is $\eta \sim 0.3$ (see Bhattacharyya, Gupta & Gil 2010), and for PSR B0943+10 $a \sim 6$ and for PSR B1822−09 $a \sim 20$, the CT is about 40 and 133 pulsar periods, respectively, which is close to what is observed. Also recently, van Leeuwen & Timokhin (2012) have argued that RS's calculation of the CT was approximate, and if the varying accelerating potential across the inner vacuum gap is considered in detail, then the slower CT can be explained. In any case, we have several lines of evidence that the CT may be upwards of three times our putative P_3 value, and for all the above reasons the corresponding 140-P_1 is not surprising. Moreover, the value is commensurate with the weak evidence that the B-mode P_3 of 70-P_1 is half the CT. This interpretation implies a carousel of three MP 'sparks' in the Q-mode and two sparks in the B-mode.

The existence of the same modulation in B1822−09's IP and MP is puzzling. Similar behaviour is also seen in two other interpulsars, B1055−52 and B1709−22 (Weltevrede, Wright & Stappers 2007; Weltevrede, Wright & Johnston 2012). In addition to having the same period, we find that a phase-locked relationship exists between the MP and IP modulation. However, the nature of the 'locking' is more complex in the present case than in the stars above as seen, for instance, in the modfold plot of Fig. 9. Focusing on the IP one can see that the intensity drops between pulse number 20 and 40 within the cycle, and the corresponding lower intensity for the MP is between about 8 and 28. This clearly shows that the IP and MP pulse sequences are offset in modulation phase by approximately 12 rotation periods – a value that is far too long to be a physical delay. More sensitive observations are needed to determine this delay accurately using cross-correlation analysis. However, a phase-locked condition exists between the IP and MP for B1822−09 as well as the other two interpulsars, signifying some information transfer between the two emission regions.

Additionally, for PSR B1822−09 the appearance of the PC signals both diminished IP and disordered MP emission, which is also an indication of information transfer. Inevitably then, we are driven to the conclusion that some kind of global magnetospheric exchange exists between the two magnetic polar regions. The current magnetospheric models of radio emission arising within the open dipolar field-line 'flux tubes' are unable to address this circumstance. In these models the out-flowing particles from the two poles stream out past the light cylinder on disconnected regions of open field. While it is possible that the CTs within the two polar regions are similar, since this depends on the surface magnetic field and rotation period, the phase-locked condition is indeed hard to understand. Weltevrede et al. (2012) discuss various physical models which can explain this phenomenon; however, their models are not developed to the extent that they can be applied to individual observations.

The focus of this work has been to characterize the peculiar moding behaviour of pulsar B1822−09 using the longest ever (37 399-pulse) continuous and sensitive single pulse observation from the GMRT. Our analysis shows that parallel IP and PC emission exist in both the pulsar's modes. The long modal intervals also allow us to accurately determine the modulation periods of the IP and MP emission, which we then use to estimate a CT for the pulsar. Finally, we emphasize that the PC emission influences mode changes in both this pulsar as well as PSR B0943+10. It is extremely important to develop theoretical conceptions regarding the origin of the PC emission. Overall, our analyses strongly suggest that mode changes entail global magnetospheric changes and information transfer between the two magnetic polar regions.

REFERENCES

Backus I., Mitra D., Rankin J. M., 2010, MNRAS, 404, 30 (Paper I)
Bhattacharyya B., Gupta Y., Gil J., 2010, MNRAS, 408, 407
Dyks J., Zhang B., Gil J., 2005, ApJ, 626, 45
Fowler L. A., Wright G. A. E., 1982, A&A, 109, 279
Fowler L. A., Morris D., Wright G. A. E., 1981, A&A, 93, 54
Gil J., Sendyk M., 2000, ApJ, 541, 351
Gil J. A. et al., 1994, A&A, 282, 45
Gil J. A., Melikidze G., Geppert U., 2003, A&A, 407, 315
Gil J. A., Haberl F., Melikidze G., Geppert U., Zhang B., Melikidze G., Jr, 2008, ApJ, 686, 497
Gould D. M., Lyne A. G., 1998, MNRAS, 301, 253
Hankins L. A., Fowler L. A., 1986, ApJ, 304, 256
Johnston S., Weisberg J. M., 2006, MNRAS, 368, 1856
Johnston S., Karastergiou A., Mitra D., Gupta Y., 2008, MNRAS, 388, 261
Mitra D., Rankin J. M., 2011, ApJ, 727, 92 (ET IX)
Morris D., Graham D. A., Sieber W., Bartel N., Thomasson P., 1981, A&AS, 46, 421
Petrova S. A., 2008, MNRAS, 384, L1
Rankin J. M., 1993a, ApJ, 405, 285
Rankin J. M., 1993b, ApJS, 85, 145
Ruderman M. A., Sutherland P. G., 1975, ApJ, 196, 51 (RS)
Suleymanova S. A., Logvinenko S. V., Smirnova T. V., 2012, Astron. Rep., 56, 207 (SLS12)
Swarup G., Ananthakrishnan S., Kapahi V. K., Rao A. P., Subrahmanya C. R., Kulkarni V. K., 1991, Curr. Sci., 60, 95
van Leeuwen J., Timokhin A. N., 2012, ApJ, 752, 155
Weltevrede P., Wright G. A. E., Stappers B. W., 2007, A&A, 467, 1163
Weltevrede P., Wright G. A. E., Johnston S., 2012, MNRAS, 424, 843

---

[1] The canonical value of $\eta \sim 0.3$ can also be understood by analysing the case of B0943+10 where the observed CT is three times longer than what is expected from the RS75 vacuum gap model. In the partially screened vacuum gap model this implies that the potential drop across the gap is three times lower giving $\eta \sim 0.3$.

This paper has been typeset from a TeX/LaTeX file prepared by the author.